Parallel fault strands at 9-km depth resolved on the Imperial Fault, Southern California

Peter M. Shearer

Institute of Geophysics and Planetary Physics, Scripps Institution of Oceanography, University of California, San Diego, La Jolla, USA

Received 10 April 2002; revised 13 June 2002; accepted 17 June 2002; published 20 July 2002.

[1] Precision relocation of hundreds of small earthquakes occurring along the Imperial Fault in Southern California during the last two decades reveals parallel steaks of seismicity at 9-km depth. These strands are spaced about 0.5 km apart within a 2 km wide zone of earthquakes near the brittle-ductile transition between the shallow locked part of the fault and a creeping zone at depth. These results suggest that the lower crustal shear zone below the Imperial Fault, site of major earthquakes in 1940 and 1979, must be at least two kilometers wide. *INDEX TERMS:* 7215 Seismology: Earthquake parameters; 7230 Seismology: Seismicity and seismotectonics; 8159 Tectonophysics: Rheology—crust and lithosphere

1. Introduction

[2] The Imperial Valley is one of the most seismically active parts of California (Figure 1). It lies at the northern end of the Salton trough in a transition region between mainly strike-slip motion along the San Andreas Fault to the north and active extension in the Gulf of California to the south. The Imperial Fault, just north of the Mexican border, was the site of major strike-slip earthquakes in 1940 (M_W = 7.1) and 1979 (M_W = 6.6), with geodetic results indicating that the fault accommodates 70% to 80% of the relative motion between the Pacific and North American plates [*Bennett et al.*, 1996; *Genrich et al.*, 1997]. Since the 1979 rupture, seismicity has mostly occurred at depths of about 7 to 11 km between the near-surface locked part of the fault and aseismic creep or distributed shear at depth [e.g., *Lyons et al.*, 2002]. The relatively shallow depth for the brittle-ductile transition zone is consistent with high heat flow observations for the Imperial Valley [*Doser and Kanamori*, 1986].

[3] Standard SCSN (Southern California Seismic Network) catalog locations for the Imperial Fault indicate a diffuse cloud of seismicity about 3 km wide. Here I apply waveform cross-correlation methods [e.g., *Nakamura*, 1978; *Poupinet et al.*, 1984; *Ito*, 1985; *Got et al.*, 1994; *Dodge et al.*, 1995; *Phillips et al.*, 1997; *Rowe et al.*, 2002] to identify clusters of similar events that can be located very accurately using differential arrival times of *P* and *S* phases. The relocated earthquakes form narrow streaks of seismicity up to 5 km long, spaced about 0.5 km apart, parallel to the surface trace of the Imperial Fault, but at a nearly constant depth of about 9 km. These results differ from previous observations of seismicity streaks in northern California [*Rubin et al.*, 1999; *Waldhauser et al.*, 1999; *Rubin and Gillard*, 2000; *Waldhauser and Ellsworth*, 2000] because the earthquakes appear to be illuminating multiple fault strands, implying that there is an active shear zone below about 10 km depth, rather than creep along a single fault plane.

0094-8276/02/2002GL015302$05.00

2. Relocation Procedure

[4] My analysis begins with *P*- and *S*-wave arrival time picks for 1454 earthquakes recorded by the SCSN between 1981 and 2000 within a 9 by 13 km box surrounding a cluster of events along the Imperial Fault (Figure 1). These are mostly small earthquakes ranging from M = 1.2 to M = 2.6. I performed initial locations using the source-specific station term (SSST) method [*Richards-Dinger and Shearer*, 2000], which improves the relative location accuracy of nearby events by applying empirical corrections for the correlated travel time residuals caused by unmodeled 3-D velocity variations. For an appropriate velocity model for the deep sedimentary basin of the Imperial Valley, I examined velocity profiles obtained by the *Fuis et al*. [1984] seismic refraction experiment. These are generally quite similar and are are characterized by a steep velocity gradient within the upper ~5 km of sediment and a shallow gradient in the metasediments above the sediment-basement interface at about 12-km depth. My *P*-wave model is derived from the closest profile to the Imperial Fault ("curve 25" from Fuis et al.). For the *S* velocities, I assume a Poisson solid below 5 km, varying smoothly to $V_S = V_P/2.37$ at the surface [*Hartzell and Helmberger*, 1982]. Results obtained with different *P* velocity profiles from *Fuis et al.* [1984] and/or assuming a Poisson solid throughout the crust are very similar to those shown here. To avoid ambiguities associated with the *Pg*/*Pn* crossover I restricted my analysis to stations within 100 km of the earthquakes (experiments with a more severe cutoff of 50 km produced results comparable to those presented here). The SSST locations have reduced scatter compared to the original catalog locations, particularly in depth, but do not resolve the streaks discussed below.

[5] Next, I collected seismograms for these events from the short-period SCSN stations and performed waveform cross-correlation to obtain *P* and *S* differential times and identify similar event clusters. To speed the computation I computed the cross-correlations only for the 100 nearest neighbors of each event, using a Delaunay tesselation of the SSST locations [*Astiz et al.*, 2000]. I identified similar event clusters as those groups of events that are connected by event pairs with an average correlation coefficient of 0.6 or

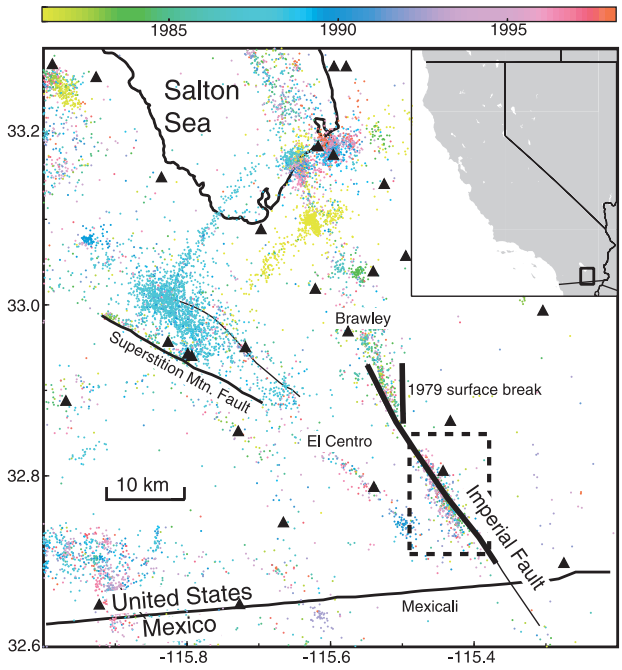

Figure 1. Recent seismicity in the Imperial Valley, California, colored by year of occurrence. The surface rupture of the 1979 M_W = 6.6 earthquake is shown as the bold line. The dotted box surrounds the cluster of events along the Imperial Fault that are the focus of this study. Seismograph locations are plotted as triangles. The inset shows the location of this figure in southernmost California.

higher [see *Shearer*, 1997, for more details]. In general, the number and size of the similar event clusters will vary depending upon the correlation coefficient cutoff used to define similarity. However, the parallel seismicity streaks that are the focus of this paper can be seen in my results for a range of different cutoff values. These similar event clusters contain 378 events (26% of my original data) in groups of 5 to 228 events. I then relocated the events within each cluster using only the differential times obtained from the waveform cross-correlation using a grid-search, L1-norm method [*Shearer*, 1998; *Shearer et al.*, 2002] that adjusts the relative location of the events in the cluster with respect to the mean cluster location. The L1-norm approach makes the method robust with respect to gross timing errors or cycle skipping in the cross-correlations. Standard errors in position are estimated from the degree of consistency between the multiple event pairs within each cluster (the solution is overdetermined). The resulting locations are shown in Figure 2. Estimated standard errors for the relative location accuracy of events within each cluster are typically less than 50 m.

3. The Seismicity Streaks

[6] Events within the similar event clusters occur in fault-parallel streaks about 0.5 km apart, at a nearly constant depth of about 9 km. These multiple streaks are unlikely to be an artifact of the location method for several reasons. They are robust with respect to changes in the assumed velocity model. Estimated relative location errors are much smaller than the ~500 m streak spacing. Errors in earthquake locations are usually greatest in depth, whereas my locations show greater separation in the horizontal direction. Finally, multiple event streaks can be seen within individual similar event clusters that are relocated with differential times alone. To test whether differences in the station distribution recording the events might artificially separate what is actually a single seismicity streak, I divided the stations randomly into two separate populations. Locations performed separately using each subset of the data continue

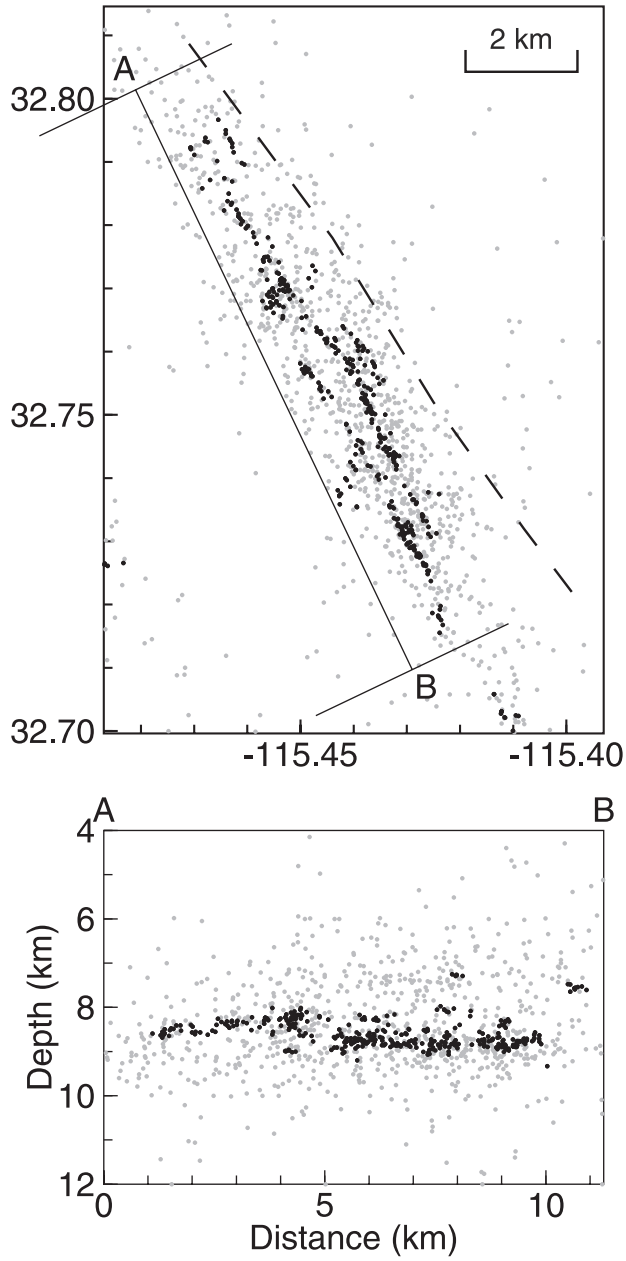

Figure 2. Locations for events along the Imperial Fault shown in map view and cross-section. The black dots indicate those events within similar event clusters that have been relocated using waveform cross-correlation. The light gray dots are the events located with arrival time picks alone. The dashed line shows the mapped surface trace of the 1979 rupture of the Imperial Fault [*Sharp et al.*, 1982].

to show multiple streaks, as do locations in which the closest four stations are excluded from the analysis.

[7] Focal mechanisms for these events are typically very poorly constrained owing to their small size and the uneven station coverage. However, *P* polarity measurements are consistent with right-lateral motion on vertical fault planes, the same type of motion that occurred during the 1979 mainshock. There is no obvious time dependence in the activity from 1983 to the present; the activity does not seem to be migrating in either position or depth. Locations for the non-similar events cannot be determined nearly as precisely as the similar events; it is possible that they also form streaks or the scatter shown in their locations might be real, indicating a diffuse zone of seismicity. The streaks are roughly parallel to the surface trace of the Imperial Fault (which ruptured in both the 1940 and 1979 mainshocks), but are displaced slightly to the southwest. The average offset is about 1 km, on the same order as the probable uncertainty in my absolute event locations. If the offset is real, then the fault plane either dips slightly at depth or recent activity is displaced from the fault plane.

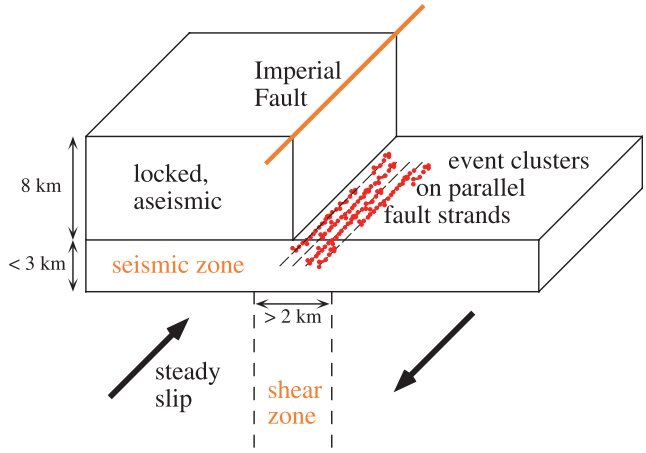

Figure 3. A cartoon showing a model of the Imperial Fault in this region that is consistent with both geodetic and seismic data.

4. Discussion

[8] The vast majority of the earthquakes occur over a narrow depth interval from 7 to 10 km (and possibly as narrow as 8 to 9 km as suggested by the similar event results). These depths are within the metasediments of the Imperial Valley, well above the basement interface at about 12 km as indicated by seismic refraction results [*Fuis et al.*, 1984]. Geodetic estimates place the bottom of the locked zone between 7.5 to 10 km [*Bennett et al.*, 1996; *Genrich et al.*, 1997; *Lyons et al.*, 2002], very close to the depth of the seismicity. Given the width of the seismogenic zone, it seems unlikely that fault creep or shear at depths below 10 km is confined to a single fault plane; rather it must be distributed within a shear zone at least 2 km wide (Figure 3). Such a model could fit available geodetic results just as well as a planar slip model.

[9] The observed streaks have some similarities to the fault-parallel lineations observed for northern California microearthquakes along the San Andreas and Hayward faults, relocated using waveform cross-correlation methods [*Rubin et al.*, 1999; *Waldhauser et al.*, 1999; *Rubin and Gillard*, 2000; *Waldhauser and Ellsworth*, 2000]. However the northern California lineations are separated vertically within a single fault plane whereas the Imperial Fault streaks are separated horizontally and apparently occur along multiple fault segments. The nearly constant depth of the Imperial streaks is similar to that seen at 3 km depth beneath Kilauea, Hawaii, where precision locations show a narrow ribbon of seismicity 2.5 km in length but less than 200 m in vertical extent [*Gillard et al.*, 1996]. These results have been plausibly modeled by Gillard et al. as representing the boundary of a locked, vertical, strike-slip fault being eroded by creep at greater depth. This model predicts that seismicity should gradually migrate with time to shallower depths.

[10] There is some evidence for a 2 to 3 km shallowing in average aftershock depths within the first few months of aftershocks following the 1979 earthquake [*Doser and Kanamori*, 1986]. However, my results indicate no change in average earthquake depth over the 1981 to 2000 time period (median earthquake depths within 5-year intervals vary by less than 0.35 km with no clear temporal trend), so any recent depth migration must be very small. SCSN arrival time data from 1979 to 1980 are not currently available. The relationship between the parallel fault planes illuminated by the microseismicity and the rupture planes of the 1940 and 1979 earthquakes is not clear. Both earthquakes broke the surface along the same fault trace so it seems likely that they also ruptured along the same fault at depth.

[11] Waveform cross-correlation provides a powerful technique for using microseismicity to image the fine-scale structure of faults. I am currently examining other faults in southernmost California to see if the results obtained for the Imperial Fault are unique to this area or reflect a more widespread phenomenon. Preliminary results suggest multiple fault strands are present along the southernmost extension of the Superstition Hills Fault, but not along the San Jacinto and Elsinore Faults to the northwest where seismicity generally extends much deeper than in the Imperial Valley.

[12] **Acknowledgments.** Personnel of the USGS/Caltech Southern California Seismic Network (SCSN) and the Southern California Earthquake Center (SCEC) were very helpful in making these data available. This work was supported by NEHRP/USGS grant 01HQGR0183 and by the Southern California Earthquake Center. SCEC is funded by NSF Cooperative Agreement EAR-8920136 and USGS Cooperative Agreements 14-08-0001-A0899 and 1434-HQ-97AG01718. The SCEC contribution number for this paper is 688.

References

Astiz, L., P. M. Shearer, and D. C. Agnew, Precise relocations and stress change calculations for the Upland earthquake sequence in southern California, *J. Geophys. Res.*, *105*, 2837–2853, 2000.

Bennett, R. A., W. Rodi, and R. E. Relinger, Global Positioning System constraints on fault slip rates in southern California and northern Baja, Mexico, *J. Geophys. Res.*, *101*, 21,943–21,960, 1996.

Dodge, D. A., G. C. Beroza, and W. L. Ellsworth, Foreshock sequence of the 1992 Landers, California, earthquake and its implications for earthquake nucleation, *J. Geophys. Res.*, *100*, 9865–9880, 1995.

Doser, D. I., and H. Kanamori, Depth of seismicity in the Imperial Valley region (1977–1983) and its relationship to heat flow, crustal structure, and the October 15, 1979, earthquake, *J. Geophys. Res.*, *91*, 675–688, 1986.

Fuis, G. S., W. D. Mooney, J. H. Healy, G. A. McMechan, and W. J. Lutter,

A seismic refraction survey of the Imperial Valley region, California, *J. Geophys. Res.*, *89*, 1165–1189, 1984.

Genrich, J. F., Y. Bock, and R. G. Mason, Crustal deformation across the Imperial Fault: Results from kinematic GPS surveys and trilateration of a densely spaced, small-aperture network, *J. Geophys. Res.*, *102*, 4985–5004, 1997.

Gillard, D., A. M. Rubin, and P. Okubo, Highly concentrated seismicity caused by deformation of Kilauea's deep magma system, *Nature*, *384*, 343–346, 1996.

Got, J.-L., J. Fréchet, and F. W. Klein, Deep fault plane geometry inferred from multiplet relative relocation beneath the south flank of Kilauea, *J. Geophys. Res.*, *99*, 15,375–15,386, 1994.

Hartzell, S., and D. V. Helmberger, Strong-motion modeling of the Imperial Valley earthquake of 1979, *Bull. Seismol. Soc. Am.*, *72*, 571–596, 1982.

Ito, A., High resolution relative hypocenters of similar earthquakes by cross-spectral analysis method, *J. Phys. Earth*, *33*, 279–294, 1985.

Lyons, S. N., Y. Bock, and D. T. Sandwell, Creep along the Imperial Fault, Southern California, from GPS measurements, *J. Geophys. Res.*, in press, 2002.

Nakamura, Y., A1 moonquakes: source distribution and mechanism, *Proc. Lunar Planet. Sci. Conf., 9th*, 3589–3607, 1978.

Phillips, W. S., L. S. House, and M. C. Fehler, Detailed joint structure in a geothermal reservoir from studies of induced microearthquake studies, *J. Geophys. Res.*, *102*, 11,745–11,763, 1997.

Poupinet, G., W. L. Ellsworth, and J. Frechet, Monitoring velocity variations in the crust using earthquake doublets: An application to the Calaveras Fault, California, *J. Geophys. Res.*, *89*, 5719–5731, 1984.

Richards-Dinger, K. B., and P. M. Shearer, Earthquake locations in southern California obtained using source-specific station terms, *J. Geophys. Res.*, *105*, 10,939–10,960, 2000.

Rowe, C., R. Aster, W. Phillips, R. Jones, B. Borchers, and M. Fehler, Using automated, high-precision repicking to improve delineation of microseismic structures at the Soultz geothermal reservoir, *Pure Appl. Geophys.*, *159*, 563–596, 2002.

Rubin, A. M., D. Gillard, and J.-L. Got, Streaks of microearthquakes along creeping faults, *Nature*, *400*, 635–641, 1999.

Rubin, A. M., and D. Gillard, Aftershock asymmetry/rupture directivity among central San Andreas fault microearthquakes, *J. Geophys. Res.*, *105*, 19,095–19,109, 2000.

Shearer, P. M., Improving local earthquake locations using the L1 norm and waveform cross-correlation: Application to the Whittier Narrows, California, aftershock sequence, *J. Geophys. Res.*, *102*, 8269–8283, 1997.

Shearer, P. M., Evidence from a cluster of small earthquakes for a fault at 18 km depth beneath Oak Ridge, southern California, *Bull. Seismol. Soc. Am.*, *88*, 1327–1336, 1998.

Shearer, P. M., J. L. Hardebeck, L. Astiz, and K. B. Richards-Dinger, Analysis of similar event clusters in aftershocks of the 1994 Northridge, California, earthquake, *J. Geophys. Res.*, in press, 2002.

Waldhauser, F., and W. L. Ellsworth, A double-difference earthquake location algorithm: Method and application to the northern Hayward fault, *California. Bull. Seismol. Soc. Am.*, *90*, 1353–1368, 2000.

Waldhauser, F., W. L. Ellsworth, and A. Cole, Slip-parallel seismic lineations on the northern Hayward fault, California, *Geophys. Res. Lett.*, *26*, 3525–3528, 1999.

P. M. Shearer, IGPP 0225, Scripps Institution of Oceanography, University of California, San Diego, La Jolla, CA, 92093-0225 USA. (pshearer@ucsd.edu)